Biophysical Chemistry 151 (2010) 170–177

Contents lists available at ScienceDirect

Biophysical Chemistry

journal homepage: http://www.elsevier.com/locate/biophyschem

The role of tryptophan in staphylococcal nuclease stability

Hong-Yu Hu [a], Ming-Chya Wu [a,b,c,*], Huey-Jen Fang [a], Michael D. Forrest [a], Chin-Kun Hu [a,d], Tian Yow Tsong [e], Hueih Min Chen [f,*]

[a] Institute of Physics, Academia Sinica, Nankang, Taipei 11529, Taiwan
[b] Research Center for Adaptive Data Analysis, National Central University, Chungli 32001, Taiwan
[c] Department of Physics, National Central University, Chungli 32001, Taiwan
[d] Center for Nonlinear and Complex Systems and Department of Physics, Chung Yuan Christian University, Chungli 32023, Taiwan
[e] College of Biological Sciences, University of Minnesota, Minneapolis, MN 55455, USA
[f] Nano Biomemdical and MEMS Technology Division, National Nano Device Laboratories, Hsinchu 300, Taiwan

ARTICLE INFO

Article history:
Received 17 May 2010
Received in revised form 8 July 2010
Accepted 12 July 2010
Available online 21 July 2010

Keywords:
Staphylococcal nuclease
W140A
F61W/W140A
Y93W/W140A
Tryptophan modification
Local hydrophobicity

ABSTRACT

Staphylococcal nuclease (SNase) has a single Trp residue at position 140. Circular dichroism, intrinsic and ANS-binding fluorescence, chemical titrations and enzymatic assays were used to measure the changes of its structure, stability and activities as the Trp was mutated or replaced to other positions. The results show that W140 is critical to SNase structure, stability, and function. Mutants such as W140A, F61W/W140A, and Y93W/W140A have unfolding, corrupted secondary and tertiary structures, diminished structural stability and attenuated catalytic activity as compared to the wild type. The deleterious effects of W140 substitution cannot be compensated by concurrent changes at topographical locations of position 61 or 93. Local hydrophobicity defined as a sum of hydrophobicity around a given residue within a distance is found to be a relevant property to SNase folding and stability.

1. Introduction

Protein folding and stability is an important and fundamental problem in biological science. In this study, we partially explore this issue by studying stability of staphylococcal nuclease (SNase) [1], a widely deployed model protein for folding study. SNase is a small, globular protein consisting of 149 amino acids residues [1] and a single Trp residue at position 140. X-ray crystallography [1–3] and nuclear magnetic resonance (NMR) [4–6] have shown that it consists of a five-stranded-barrel and three α-helices (Fig. 1). SNase has an N-terminal β-core and a C-terminal sub-domain as two independently folding segments. The generation of the interactions between the two sub-domains is crucial in SNase folding [7–12].

Recently, analysis of mutant proteins with amino acid deletions/substitutions [13–16] shows that mutant SNase with a C-terminal deletion [17] or lacking of the C-terminal 13 residues (Δ137–149) [18], folds to a compact non-native state, even under physiological conditions. This state is structurally similar to an early folding intermediate [19,20] and it is believed that these residues contain information critical to the native folding of SNase, especially to the interaction between N-terminal and C-terminal sub-domains. Among the residues 137–149, the importance of Trp at position 140 (see Fig. 1) has been highlighted by substitution studies [21,22]. It was also showed that only W140H, W140F and W140Y have conformations and activities similar to the wild type (WT) SNase [23]. Nevertheless, mutants with alternative amino acid substitutions at position 140, for example W140A, assume a compact non-native structure similar to the Δ137–149 deletion mutant [24]. This suggests that side chain information encoded by residue 140 is essential to native folding. It must be a five- or six-member ring structure, and among which Trp provides the most suitable ring. The ring structure is integral to the formation of a C-terminal cluster [3]. Formation of the cluster generates long-range interaction connecting the C-terminal segment with the N-terminal β-core section, which is fundamental to the native global confirmation.

In this study we went further to confirm that W140 is a key residue in determining the structure and function of SNase. Circular dichroism (CD), intrinsic and 8-anilino-1-naphthalensulfonate (ANS)-binding fluorescence, chemical titrations and enzymatic assays were used to assay the structure, stability and activities of WT SNase and its mutants, W140A, F61W/ W140A and Y93W/W140A. Both Phe and Tyr have most required properties of Trp such that they can be used to address the issue of position-dependence of Trp in SNase.

* Corresponding authors. Wu is to be contacted at Research Center for Adaptive Data Analysis, National Central University, Chungli 32001, Taiwan.
E-mail addresses: mcwu@ncu.edu.tw (M.-C. Wu), hmchen@ndl.org.tw (H.M. Chen).

0301-4622/$ – see front matter © 2010 Elsevier B.V. All rights reserved.
doi:10.1016/j.bpc.2010.07.001

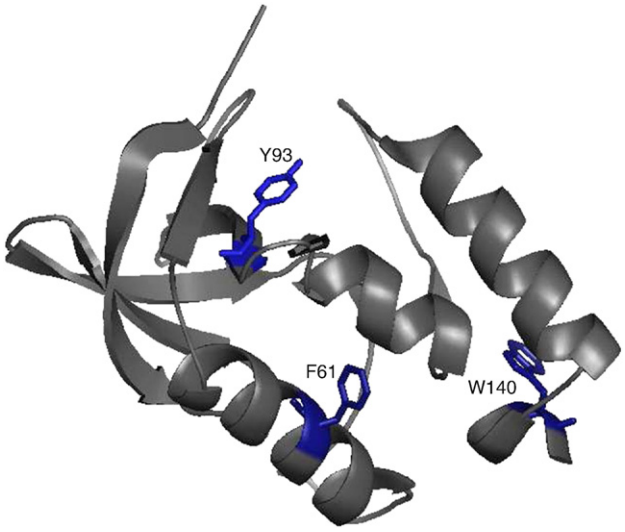

Fig. 1. Cartoon diagram of wild-type staphylococcal nuclease (PDB code 1EY0). The side chains of F61, Y93, and W140 are highlighted with blue stick representations. (For interpretation of the references to color in this figure legend, the reader is referred to the web version of this article.)

Further considerations were based on hydrophobicity (HP) [25] (HP: Phe>Trp>Tyr) and topographical concern of the loop interaction of the regions at 61 (loop 3 shown in [26] is surrounded by a helix) and 93 (loop 2 shown in [26] is surrounded by sheets) (see Fig. 1). The designation facilitates the test of the folding model of SNase, in which the nucleation process is assumed in the early folding stage. We propose that such nucleation is controlled by two factors, one being the properties of Trp and the other being the position of key amino acid residue like Trp. Our results show that comparing with WT, all mutants above have unfolding, corrupted secondary and tertiary structure, diminished structural stability and attenuated catalytic activity. On this basis, we conclude that W140 is critical to SNase conformational integrity, stability and function. F61W or Y93W substitution is unable to counter the deleterious effects of W140A.

2. Materials and methods

2.1. Materials

The WT SNase *nuc* gene was originally donated by Prof. David Shortle. Luria–Bertani broth and isopropyl-1-thio-β-D-galactopyranoside were purchased from Difco Laboratories and Sigma, respectively. Salmon testes DNA and some analytical grade chemicals such as EDTA, Tris–HCl, $CaCl_2$, NaCl, and mineral oil were obtained from Sigma. Salmon testes DNA was used without further purification. Guanidine hydrochloride and dNTPs were purchased from Roche Molecular Biochemicals. Absolute ethanol (>99%) was obtained from Panreac, and urea was a product of Acros. The Stratagene QuickChange™ kit containing *Pfu* DNA polymerase, 10× reaction buffer, and *Dpn*I restriction enzyme was purchased from Stratagene. The 2-Methyl-2,4-pentadiol was purchased from Merck. Water used for these experiments has been deionized and distilled.

2.2. Site-directed mutagenesis

Mutants used for this experiment were generated by the PCR site-directed mutagenesis method. A commercial kit (Stratagene QuickChange™) was used for sample preparation. Trp 140 was replaced by Ala. Phe 61 and Tyr 93 were replaced by Trp. Plasmid pL9 encoding WT SNase was stored at −20 °C before mutagenesis. Two complementary 33-mer primers that include the Ala codon at position 140 and Trp codon at position 61 or 93 were designed and synthesized (Life Technologies, Inc.). A single point mutation was made to generate W140A. Double mutation was used to generate F61W/W140A and Y93W/W140A by using a single point mutation plasmid as a template. The PCRs were then conducted. After isolation of DNAs, the mutants were identified by cutting with restriction endonucleases, *Nco*I and *Bam*HI. The mutant sequences (positions 1–149) verified by an automated DNA sequencer (ABI PRISM 310 Genetic Analyzer) were compared to the WT sequence and were found to be correct.

2.3. Protein purification

Colonies picked from −80 °C storage bottles containing WT or mutant SNase expression plasmids were streaked on ampicillin-containing agar plates. The plates were incubated at 37 °C overnight. One colony from each plate was isolated and then inoculated into 2 ml LB medium containing ampicillin, and the culture was incubated at 37 °C at 250 rpm for 5 h in a shaker incubator. A small amount of cell medium was poured into a 1-liter flask containing 200 ml LB medium. The flask was incubated in the shaker incubator at 37 °C, 250 rpm overnight. Five portions of 40 ml cell culture were then poured into each of five 1-liter flasks containing 400 ml of LB medium. These flasks were again incubated in the shaker incubator at 37 °C at 250 rpm for 4 h. Isopropyl-1-thio-β-D-galactopyranoside (20 μl, 0.5 mM) was added to each flask and then incubated for 4 h to induce recombinant protein expression. Cells were harvested at 4 °C by centrifugation at 4000 rpm for 15 min. Supernatant was discarded. The pellets were slowly dissolved by adding buffer A (6 M urea, 1 mM EDTA, 0.2 M NaCl, 50 mM Tris–HCl, pH 9.2). The solution was centrifuged at 1000 rpm for 15 min. The supernatant was then mixed with prechilled absolute ethanol (1:1, v/v). The mixture was incubated at −20 °C for 2 h and was centrifuged at 4 °C, 7500 rpm for 20 min. The sediment was discarded. The remaining liquid was mixed with prechilled absolute ethanol (1:2, v/v) and incubated at −20 °C overnight. After proteins being completely precipitated, the sample was centrifuged at 1000 rpm for 15 min, and the supernatant was discarded. The pellets were then dissolved in buffer B (6 M urea, 1 mM EDTA, 50 mM Tris–HCl, pH 9.2). Further purification was conducted using a cation exchange column (Carboxy-Methyl-25). The column was loaded with protein solution and washed with buffer B. The sample was eluted with buffer C (6 M urea, 1 mM EDTA, 1 M NaCl, 50 mM Tris–HCl, pH 9.2) and collected by a fraction collector measuring absorbance at 280 nm. The purified proteins were dialyzed with distilled water and then lyophilized by a vacuum freeze dryer. The yield of proteins was ~40 mg/l. The purities were checked by 15% SDS-PAGE with Coomassie Blue stain. A purity of over 90% was estimated by densitometry (Molecular Dynamics, Inc., Sunnyvale, CA). The protein extinction coefficients were calculated with Gill and von Hippel's method [27].

2.4. Enzyme activity assay

Enzyme activity was determined by incubating the enzyme with a DNA substrate and measuring the change of absorbance at 260 nm. 50 μg substrate DNA was dissolved in 1 ml buffer (10 mM $CaCl_2$, 25 mM Tris–HCl, pH 8.8). The mixture was boiled for 30 min and then cooled on ice for 15 min. 5 μl enzyme (1 mg/ml) was gently mixed with 1 ml substrate buffer in a spectrophotometer cuvette. The change in absorbance at 260 nm was recorded as a function of time. Nonlinear regression analysis was used to calculate best-fit curves of V_0 versus [C], where V_0 is the initial velocity and [C] is the substrate concentration. The Michaelis constant, K_m, and the maximal velocity, V_{max}, were calculated from the best-fit curves.

2.5. CD spectroscopy

WT and mutant protein solutions were prepared in a phosphate buffer (1 mg/ml) for CD studies with a J-720 spectropolarimeter (Jasco). The CD spectra were recorded in the far-UV region (200–250 nm) by using a 1-mm path length cuvette with capacity 200 μl. The data obtained from Jasco J-720 was transferred to Origin™ software (MicroCal Software, Inc.) for plotting and further processing. A series of experiments were conducted by observing the shifts of CD at 222 nm for pH from 2.0 to pH 8.0 and for denaturant (guanidine hydrochloride, Gdn-HCl) concentrations from 0 M to 2 M. For pH-shifting experiments, the solution pH was adjusted to the desired value by using 6 M HCl or 5 M NaOH. For Gdn-HCl experiments, the final solution was prepared by diluting 6 M Gdn-HCl stock solution with a protein solution to the desired concentrations. Each experiment was completed by 10–15 samples for different conditions.

2.6. Fluorescence spectroscopy

Protein solutions in a phosphate buffer (1 mg/ml) were prepared for fluorescence studies with a luminescence spectrometer LS50B (Perkin-Elmer Life Sciences). The fluorescence spectra were recorded at wavelengths from 300 nm to 550 nm and excitation at 298 nm by using a 1-cm path length cuvette with capacity 700 μl. The data obtained from the LS50B fluorometer were transferred to Origin™ software for plotting and further processing.

2.7. NBS modification of tryptophan

Protein species (WT, Y93W/W140A) were incubated in the dark with *N*-Bromosuccinimide (NBS) solution. Solutions differing in their molar ratio of NBS/protein were prepared. These mixtures were stirred at room temperature for more than 30 minutes and then assayed by fluorescence spectroscopy and far-UV CD. Reaction constants for NBS oxidation were calculated from fluorescence data according to pseudo-first-order kinetics.

2.8. TFE helical induction experiments

Solutions were prepared by dissolving particular protein species (WT, W140A, Y93W/W140A) in a buffer containing 10 mM phosphate, 50 mM NaCl and variable trifluoroethanol (TFE) concentration. A second set of the same solutions were set to pH 2.1 by HCl addition. $[\theta]_{222\ nm}$ was assayed for the solutions.

3. Results

3.1. CD spectra of SNase and mutants

Far-UV CD spectra for WT and mutants were shown in Fig. 2A. Negative peaks at 208 and 222 nm were indices of a protein's α-helical content [28,29]. The peaks for W140A at $[\theta]_{222\ nm}$ are not so pronounced as that for WT, indicating that W140A has a lower α-helical content than WT. In this context, the CD spectra of F61W/W140A and Y93W/W140A are closer to WT, suggesting greater similarity to WT in terms of α-helical content. Table 1 summarizes the secondary structure compositions of WT, W140A, F61W/W140A and Y93W/W140A. The mutants are different from WT in descending order of disparity: W140A>Y93W/W140A>F61W/W140A. WT has the same percentage content of α-helix as β-sheet, while all the mutants have less α-helix than β-sheet. Mutant percentage α-helix decreases with the increase of percentage β-sheet in the order of disparity. The decrement of the α-helical content is 50% (for Y93W/W140A) to 70% (for W140A) of the original in WT, and the increment of the β-sheet content is 25% (for F61W/W140A) to 135% (for W140A) of the original in WT. W140A even has twice the percentage β-sheet of WT. All the mutants have a lower percentage composition of turns than WT. The percentages of turn in mutants follow in decline the same order of disparity from WT.

Near-UV CD spectra are shown in Fig. 2B for WT and mutants. Ellipticity in the near-UV region around 277 nm reflects the asymmetry of the environment of aromatic groups and is an index of the uniqueness of the protein tertiary structure. Fig. 2B shows that all the mutants have very different tertiary structure from WT. The descending order of disparity is: Y93W/W140A>F61W/W140A>W140A. F61W/W140A have similar tertiary structure contents, but that of Y93W/W140A is very different.

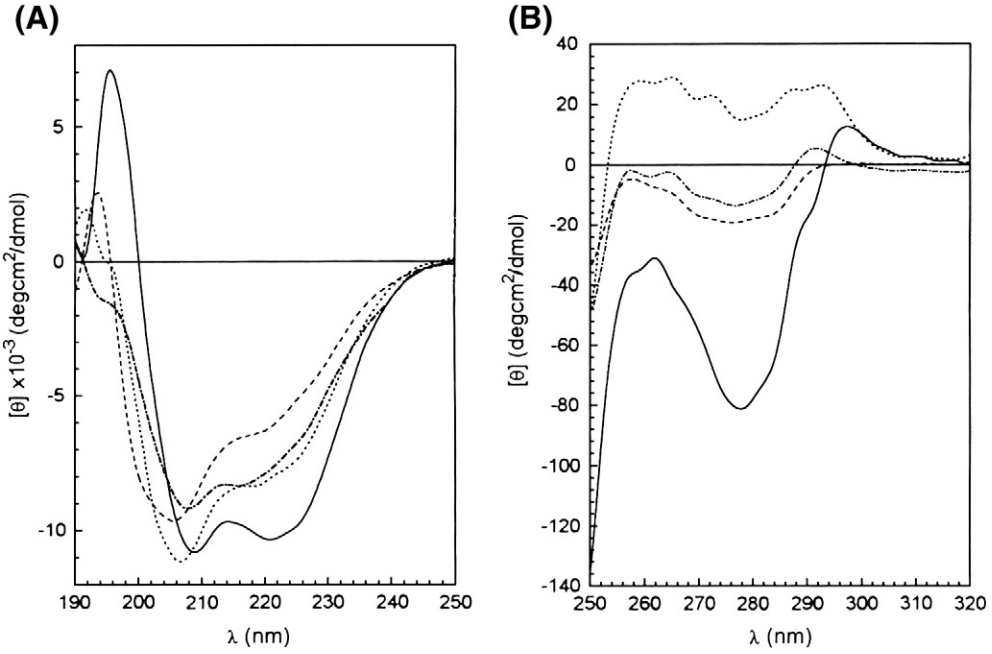

Fig. 2. CD spectrums of WT and mutants. (A) Far-UV CD spectrum: WT SNase (solid), W140A (dashed), F61W/W140A (dashed and dotted) and Y93W/W140A (dotted); (B) Near-UV CD spectrum: WT SNase (solid), W140A (dashed), F61W/W140A (dashed and dotted) and Y93W/W140A (dotted).

Table 1
Secondary structure of SNase and its mutants as estimated from far-UV CD spectra.

Structure	WT	W140A	F61W/W140A	Y93W/W140A
Helix (%)	23.1	6.7	15.6	12.9
Sheet (%)	23.2	52.4	29.0	38.4
Turn (%)	22.1	4.3	17.7	11.8
Random (%)	31.6	36.6	37.7	36.9

3.2. Enzymatic activity of SNase and mutants

Table 2 shows the Michaelis–Menten kinetic parameters for WT and mutants, with DNA substrate. All the mutants have higher Michaelis–Menton constants, K_m, and lower maximum reaction rates, V_{max}, implying impaired enzymatic activity in comparison with WT. Note that all the mutants have the same value of K_m, within the margin of experimental error. W140A and F61W/W140A have the same value of V_{max}. Whilst Y93W/W140A has a slightly greater value, it is only 31% of the WT.

3.3. Gdn-HCl induced unfolding of SNase and mutants

The first row of Table 3 lists the fractional fluorescence intensities of SNase and its mutants with Gdn-HCl, which indicates Gdn-HCl induced fractional changes in tertiary structures. The second row of Table 3 are fractional $[\theta]_{222\ nm}$ of SNase and its mutants with Gdn-HCl. They are Gdn-HCl induced fractional changes in α-helical contents. The third row of Table 3 shows fractional enzymatic activity for SNase and its mutants with Gdn-HCl. There is no tryptophan in W140A. The intrinsic fluorescence is contributed by the 7 Tyrosines and 3 Phenylalanines which have relatively lower intensity. The significant differences between fluorescence measurement and far-UV $[\theta]_{222\ nm}$ measurement are due to the fact that the deletion of the tryptophan leads to a corrupted structure which reduces the intrinsic fluorescence to a significant amount, while the whole system (including folding intermediates) is substantially in a compact dimension [12,30]. This scenario is more apparent in the case of mutant W140A. Comparing with the data in Table 2, here WT has the least relative loss of secondary (α-helical contents) and tertiary structures, but the greatest relative activity loss. In contrast, W140A has the greatest relative secondary and tertiary structure loss, but the least relative activity loss. Thus residual activity is more resilient to Gdn-HCl than WT's full activity. F61W/W140A has slightly less relative tertiary structure intact than Y93W/W140A, but greater relative activity. The Gdn-HCl assays assign order of structural stability, with WT being the most stable, W140A the least, and the double mutants in between. Consequently, for individual protein species, the degree of relative activity loss correlates with relative structural loss. This is not the case for different protein species.

3.4. ANS-binding fluorescence spectra of SNase and its mutants

ANS amplifies the fluorescence on binding hydrophobic surfaces or clusters, such that it can be used as a structural probe to assay changes in the surface HP of proteins. A greater ANS fluorescence intensity implies greater exposure of hydrophobic side chains in the nuclease, suggesting partial unfolding of the molecule. Fig. 3 shows the fluorescence emission spectra of ANS in the presence of SNase and its mutants. Hydrophobic side chains are normally buried in native protein structures. All the mutants exhibit significant unfolding as compared to WT. The order is, starting with the most unfolded, Y93W/W140A>W140A>F61W/W140A.

Table 2
Comparative activities of SNase and mutants.

Protein	WT	W140A	F61W/W140A	Y93W/W140A
K_m (μg/ml)	69 ± 0.64	10.17 ± 0.29	10.06 ± 0.60	10.23 ± 0.59
V_m (min^{-1}(μg/ml)$^{-1}$)	4.73 ± 0.03	1.06 ± 0.01	1.12 ± 0.11	1.46 ± 0.04
%	100	22	24	31

Table 3
Mid-point transition of SNase and mutants by Gdn-HCl unfolding.

Protein	WT	W140A	F61W/W140A	Y93W/W140A
Fluorescence (Cm;M)	0.82 ± 0.06	0.15 ± 0.02	0.63 ± 0.05	0.64 ± 0.04
Far-UV θ_{222} (Cm;M)	0.80 ± 0.04	0.45 ± 0.02	0.55 ± 0.04	0.50 ± 0.03
Activity (50%;M)	0.4 ± 0.05	0.15 ± 0.02	0.12 ± 0.01	0.09 ± 0.01

3.5. NBS-binding fluorescence and far-UV spectra of WT and Y93W/W140A

Covalent modification of amino acid side chains is a technique usually used to investigate the structure-function relationships of specific residues in proteins. NBS modification of Trp oxidises its indole group to oxindole; possibly altering its local environment and disrupting the indole group's hydrogen bonding to other groups on the main or side chains. NBS modification can thus cause protein structural changes. In the experimental conditions we used, NBS can only access and modify relatively exposed Trps. Fig. 4A shows the far-UV CD spectra of WT for different molar ratios of NBS/protein. The greater the ratio is, the smaller is $[\theta]_{222\ nm}$. NBS disrupts WT α-helical structure, suggesting W140 is integral to this structure. When the molar ratio equals 40, the far-UV CD spectrum is very similar to that of W140A.

Trp has intrinsic fluorescence [31]. NBS oxidation of the indole chromophore switches it from absorbance at 280 nm to 250 nm. WT and Y93W/W140A both have a single Trp residue. Fig. 4B shows the fluorescence intensity of WT and Y93W/W140A as a function of [NBS]/[protein]. Higher ratios yield lower fluorescence intensities, whereas this relationship saturates at ratio 20 for Y93W/W140A, and 30 for WT. Y93 in Y93W/W140A is likely more exposed than W140 in WT. Fig. 5A shows the fluorescence intensity of WT and Y93W/W140A, Fig. 5B the $[\theta]_{222\ nm}$ of WT, for different [NBS]/[protein] ratios, as a function of reaction time. With excess NBS, pH 7.4 and at 25 °C, the NBS binding rate constants are $(2.51 \pm 0.20) \times 10^{-3}\ s^{-1}$ for WT and

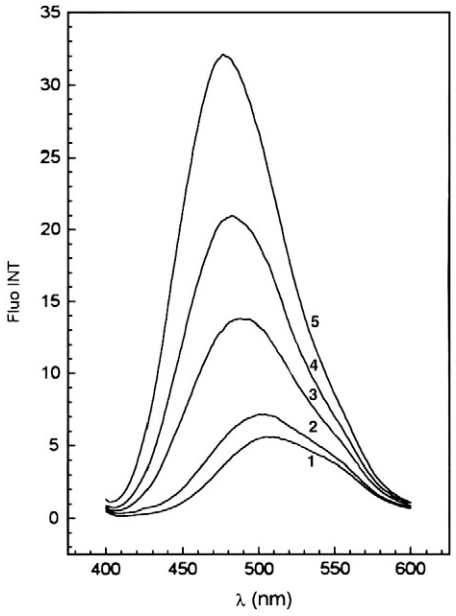

Fig. 3. Fluorescence emission spectra of ANS in the presence of SNase and its mutants. Curves 1–5: (1) ANS only, (2) WT, (3) F61W/W140A, (4) W140A and (5) Y93W/W140A.

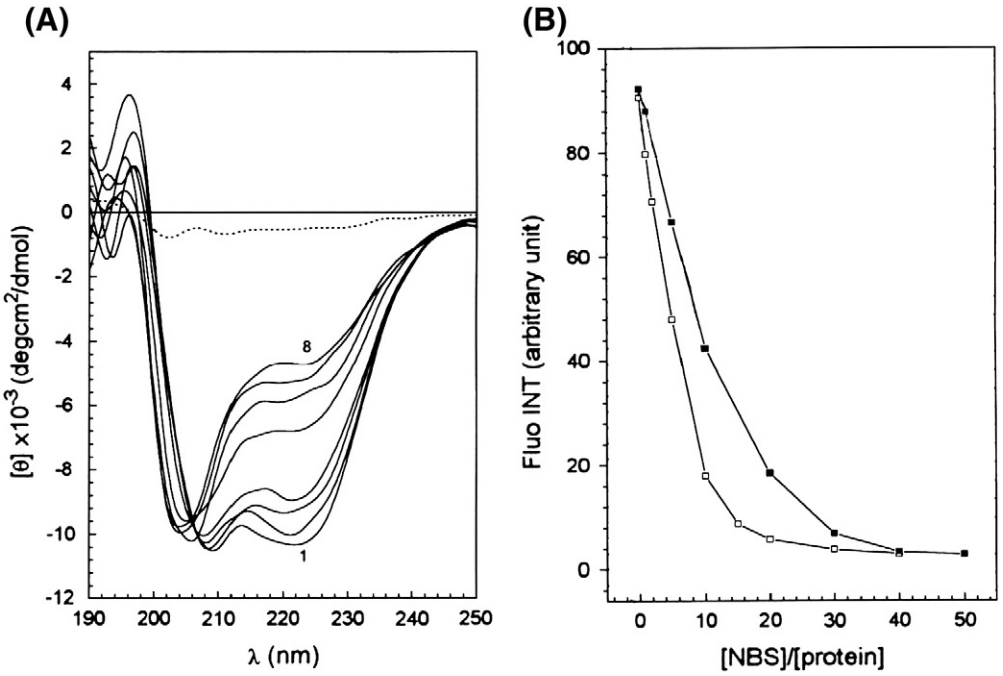

Fig. 4. Equilibrium modification of WT and Y93W/W140A by NBS. (A) Far-UV CD spectra of WT for different molar ratios of NBS/protein. The ratios are 0, 1, 5, 10, 20, 30, 40, and 50 for lines 1–8 respectively. The dotted line is NBS only; (B) Fluorescence intensity of WT and Y93W/W140A as a function of [NBS]/[protein]. WT SNase (solid square) and Y93W/W140A (open square).

$(7.39 \pm 0.06) \times 10^{-3}\ s^{-1}$ for Y93W/W140A. NBS can more readily modify Y93 in Y93W/W140A than W140 in WT. Thus, Y93 in Y93W/W140A is likely more exposed than W140 in WT.

3.6. TFE titrations monitored by CD

TFE concomitantly weakens hydrophobic interactions and strengthens local hydrogen bonds between residues closured in the amino acid sequence, stabilizing secondary structure motifs. Fig. 6A shows $[\theta]_{222\ nm}$ for WT, W140A and Y93W/ W140A at pH 7.4, as a function of TFE concentrations in percentage (v/v). We have shown in Section 3.2 that W140A and Y93W/W140A have less α-helical content than WT. TFE proportionally increases the α-helical content of W140A and Y93W/W140A; at around 13%–14% TFE, they have the same α-helical content as WT. WT α-helical content is only increased with >17% TFE. Thus, hydrophobic interaction play an essential role in folding of these molecules. Fig. 6B shows $[\theta]_{222\ nm}$ for WT and W140A at pH 2.1, as a function of TFE concentrations in percentage (v/v). TFE proportionally

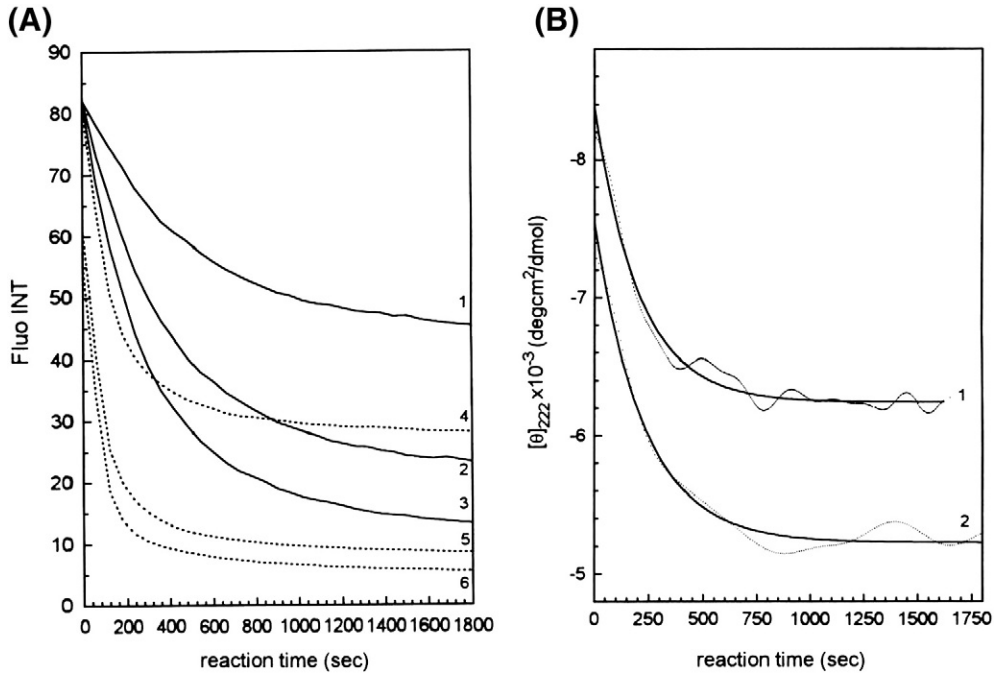

Fig. 5. Kinetics of NBS oxidation of the tryptophan residue in WT and Y93W/W140A. (A) Fluorescence intensity of WT (solid) and Y93W/W140A (dotted). [NBS]/[protein] ratio is 10, 20, and 30 for lines 1, 2, 3 and 4, 5, 6 respectively; (B) $[\theta]_{222\ nm}$ for WT SNase. Lines 1 and 2 refer to [NBS]/[protein] ratios of 20 and 30 respectively.

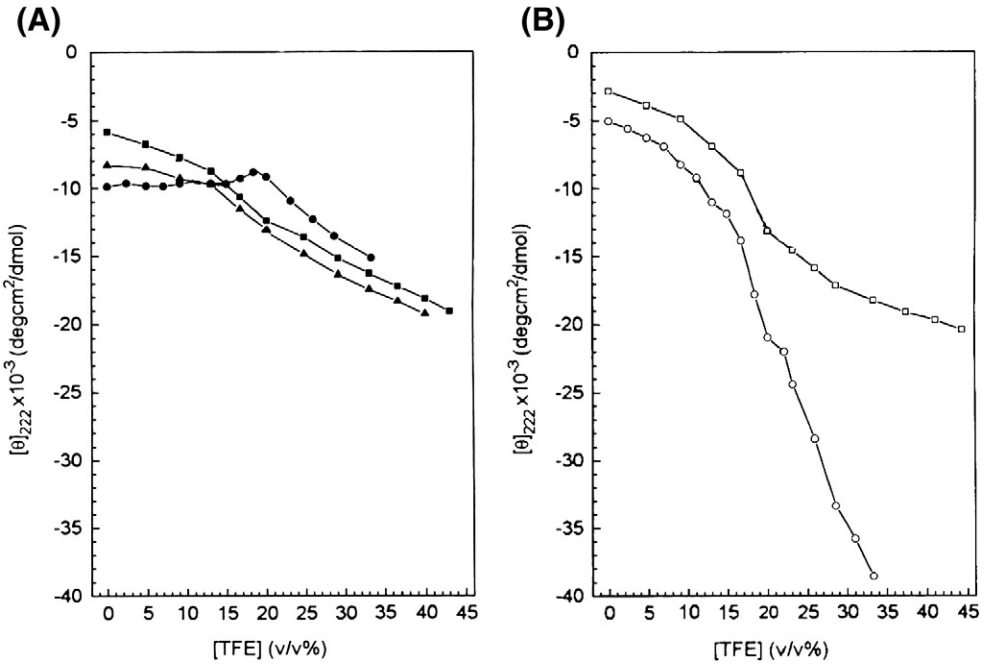

Fig. 6. $[\theta]_{222\ nm}$ for WT, W140A and Y93W/W140A as a function of TFE concentrations in percentage (v/v). (A) At pH 7.4. WT SNase (circle), W140A (square), and Y93W/W140A (triangle); (B) At pH 2.1: WT SNase (circle) and W140A (square).

increases the α-helical content of WT and W140A, although much less for W140A. The TFE induced changes at pH 2.1 are much greater than those at pH 7.4.

4. Summary and discussions

4.1. W140 is critical to SNase structure and function

According to our far-UV CD, near-UV CD and enzymatic assays, mutant W140A has unfolding, corrupted secondary and tertiary structures, diminished structural stability and attenuated catalytic activity compared to WT SNase. When the Trp at position 140 is shifted to other locations even in the loop interaction areas (such as at positions 61 and 93, see Ref. [26]), the mutants have impaired structures and enzymatic activities. NBS-binding fluorescence and far-UV spectra measurement suggests that W140 is integral to the structure, while it is more exposed in the mutants. These observations suggest that Trp at position 140 is a "key" residue to SNase conformational integrity, stability, and function. When Trp is not at position 140, it is not a key residue anymore. Gdn-HCl induced unfolding of WT SNase and mutants shows that for individual mutants, the degree of relative activity loss correlates with relative structural loss, but this is not the case for different mutants. Consequently, ANS-binding fluorescence spectra suggests that unfolded degree is Y93W/W140A>W140A>F61W/W140A, whilst the comparative activities for the mutants are: Y93W/W140A>F61W/W140A>140A. Furthermore, TFE titrations monitored by CD confirm that hydrophobic interactions play essential roles in secondary structure formations of these molecules. From these results, we can now draw a general picture for the role of Trp at position 140 in SNase.

Within the interaction region centered at the Trp of position 140, other possible residues contribute to the internal forces interacting with this residue and underpinning the protein structural frame. According to the X-ray structure of SNase, W140 is an important residue for hydrophobically assembling an influential local C-terminal cluster, mainly comprising G107, K110, E129, A132, K133 and I139 [2] (see Fig. 7A). This cluster is formed in early folding stage. This and other local clusters latter generate long-range interactions connecting the C-terminal sub-domain with the N-terminal β-core sub-domain. These interactions are fundamental to the native global conformation. In this way, W140 is integral to both short-range and long-range structural interactions in a hierarchical fashion. The local C-terminal

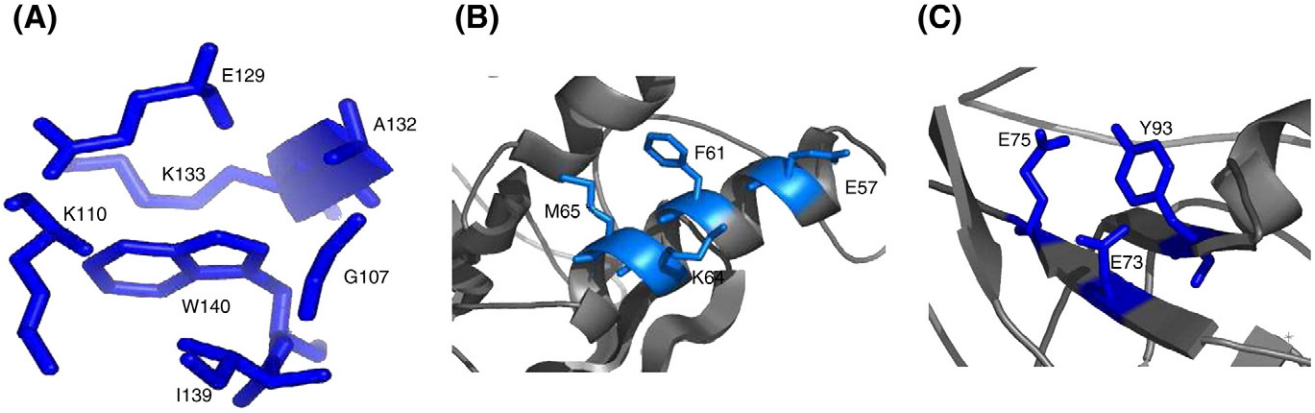

Fig. 7. The residues around Trp 140, Phe 61 and Tyr 93. (A) The residues around Trp 140; (B) The residues around Phe 61; (C) The residues around Tyr 93.

cluster is centered at W140's five-member ring, which contacts I139 and W140 at the C-terminal loop, A132 and K133 at the end of the C-terminal α-helix and G107 at the second short α-helix of the end of C-terminal. W140's six-member ring also possibly contacts both K110 and E129. The hydrophilic cluster groups are located on the aqueous exposed cluster half. The other cluster half, which is relatively hydrophobic, interacts hydrophobically or through van der Waals interactions with the N-terminal sub-domain, especially Y54 and P42 residues [2,21]. Such a configuration finally contributes to the profile of local hydrophobicity (LHP) shown in Fig. 8, in which the last two helices are in a relatively more hydrophilic environment suitable for the C-terminal cluster. W140A substitution is structurally disruptive because Ala does not have the required ring to seed the cluster. The resultant disordered cluster formation corrupts the long-range interactions connecting the C-terminal sub-domain with the N-terminal β-core sub-domain and disorganizing tertiary structure. Since the component residues, R35, Y85, R87, Y113 and Y115, distributed from the N-terminal domain to the C-terminal sub-domain [3] are very sensitive to these interactions, it distorts active site conformation and in turn negatively impacts enzymatic activity.

4.2. The effect of two topographically different double-mutation

The double mutants created with double-mutation (W→A/ F→W or W→A/Y→W) at positions 61 and 93, which are at topographically different interaction regions, are not systematically more similar or different to WT, than W140A is to WT. The deleterious effects of a W140A substitution cannot be compensated by a concurrent F61W or Y93W substitution. W140 seeds the structurally crucial C-terminal cluster, but W61 and W93 likely cannot. A crucial factor could be different Trp environment. W93 in Y93W/W140A is more medium exposed than W140 in WT. The LHP estimated by the evaluation of Trp substitution by Phe at 61 and Typ at 93 shows that these substitutions cannot reproduce a similar profile of LHP to have the WT configuration [32] (see Fig. 9 and discussions below). The folding pathway is changed due to different environments in early nucleation processes [30].

While the W140A mutant adopts a random coil conformation, F61W and Y93W substitutions generate novel interactions to provide additional structure and stability to W140A mutants. This is most pronounced for the Y93W substitution. Y93W confers a non-native, rearranged tertiary conformation to W140A mutant. The interactions of F61 and Y93 are shown in Fig. 7B and C, respectively. The high resolution SNase crystal structure (PDB 1SNC) locates Phe 61 in the middle of the α-1 helical domain, backbone hydrogen bonding with F61, M65, E57 and K64 (Fig. 7B). Trp at position 61 provides a similar stereo aromatic side chain to the native Phe, but less hydrophilic. Tyr 93 is located in the

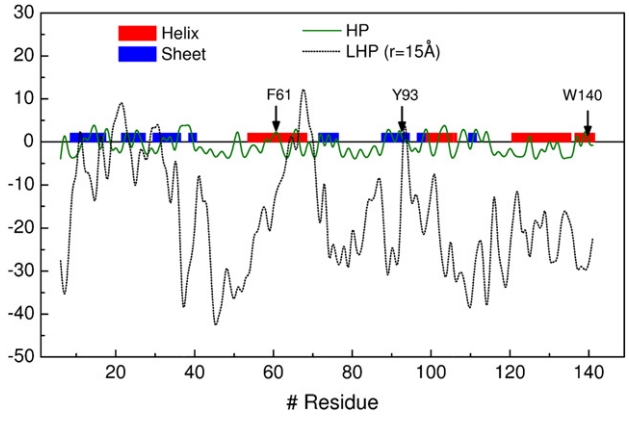

Fig. 8. Hydrophobicity (HP) and local hydrophobicity (LHP) of the PDB protein structure 1EY0 according to the Kyte–Doolittle scale [25]. The LHP is defined in Eq. 1 as the sum of HP of surrounding residues within a range of $r = 15$ Å. Locations of F61, Y93 and W140 are indicated by arrows.

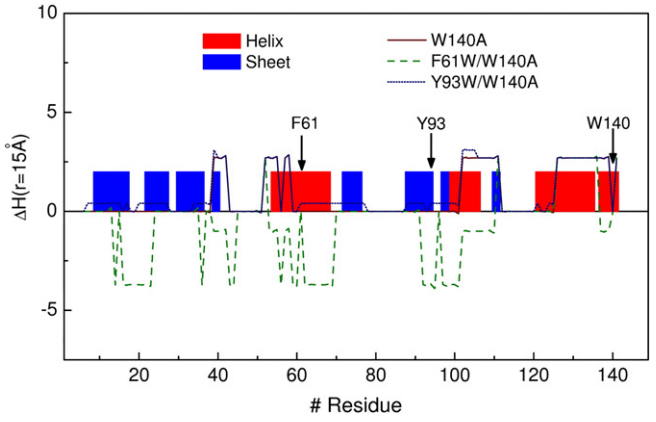

Fig. 9. Changes of the LHP in mutants with respect to the WT SNase for W140A, F61W/W140A, and Y93W/W140A.

middle of the β5-strand, side-chain hydrogen bonding with E75 and backbone hydrogen bonding with E73 (Fig. 7C). Trp at position 93 confers more hydrophilicity and a very different hydrogen bonding profile to Tyr, resulting in structural rearrangements between K9, E75, Y93 and H121 [33].

4.3. Interpretations in terms of LHP

Above observations for the trends of the changes of secondary structure contents in mutants listed in Table 1 can be interpreted by the changes of protein's LHP. Here LHP is defined as a sum of hydrophobicities [25] of residues around a given reside within certain distance. For a given protein chain consisting of N residues, we calculate the LHP of the i-th residue H_i by

$$H_i = \sum_{\langle i,j \rangle} S_j e^{r_{ij}/r}, \tag{1}$$

where $\langle i,j \rangle$ indicates that the distance r_{ij} between pair residues i and j is less than r which defines the effective range of LHP, and S_j is HP of the j-th residue. In Eq. 1, we also assume an exponential decay of the strength of HP with respect to r. Fig. 8 shows a typical LHP calculation of WT SNase with $r = 15$Å, as a function of residue number. For mutant W140A, we replaced Trp at 140 by Ala and calculated the corresponding LHP by Eq. 1. The change of LHP can then defined as

$$\Delta H_i(\text{mutant}) = H_i(\text{mutant}) - H_i(WT), \tag{2}$$

and the results of three mutants are shown in Fig. 9. Note that, the relatively lower percentage of helix in W140A than in WT SNase is consistent with the increase of LHP around 54–58 and 103–106 due to the substitution of Trp by Ala. Consider the conformation of a mutant as a folding intermediate state of WT. According to the energy minimization criterion, the intermediate state tends to fold toward a new conformation with lower potential energy. The increase of LHP is then compensated by unfolding or diminishing the second helix in the N-terminal and two helices in the C-terminal. Meanwhile, the increase of the content of sheets in W140A SNase is likely due to the preservation of sheet structures formed in the early nucleation and without a harmony with the interaction of Trp at 140 in later hierarchical assembly [30]. The same inference based on the changes of LHP can be applied to illustrate the scenarios of F61W/W140A and Y93W/W140A mutants (see Fig. 9). The decrease of LHP in F61W/W140A is compensated by more closely packing of the portions of helices and sheets in lower local hydrophobicities. However, the absence of Trp at position 140 fails to seed the nucleation in the C-terminal cluster such that the percentage of helix content of F61W/W140A is still lower than WT. The situation for Y93W/W140A is different. More portions of Y93W/W140A tend to unfold to

compensate the increase of LHP. It follows that unfolded degree is Y93W/W140A>W140A>F61W/W140A, which is consistent with the fluorescence emission spectra of ANS shown in Fig. 3. Moreover, Trp probably has a stronger influence than Phe and Tyr on the nucleation and facilitates formation of surrounding secondary structures. Thus, mutant F61W/W140A has more helix content than W140A, while mutant Y93W/W140A has more sheet content than F61W/W140A. Mutant Y93W/W140A has less sheet content than W140A due to the compensation of the increase of LHP around sheets [32].

Acknowledgements

This work was supported by the National Science Council of the Republic of China (Taiwan) under Grant Nos. NSC 96-2112-M-008-021-MY3, 97-2627-B-008-004 and 98-2627-B-008-004 (M.-C. Wu), 96-2911-M-001-003-MY3 (C.-K. Hu), and 95-2320-B-001-019 (H.-M. Chen), National Center for Theoretical Sciences in Taiwan, and by Academia Sinica (Taiwan) under Grant No. AS 95-TP-A07.

References

[1] F.A. Cotton, E.E. Hazen, M.J. Legg, Staphylococcal nuclease: Proposed mechanism of action based on structure of enzyme-thymidine 3′, 5′-bisphosphate-calcium ion complex at 1.5-Å resolution, Proc. Nat. Acad. Sci. U.S.A. 76 (1979) 2551–2562.
[2] P.J. Loll, E.E. Lattman, The crystal structure of the tertiary complex of staphylococcal nuclease, Ca^{2+} and its inhibitor pdTp, refined at 1.65 Å, Proteins 23 (1989) 115–124.
[3] J. Chen, Z. Lu, J. Sakon, W.E. Stites, Increasing the thermostability of staphylococcal nuclease: implications for the origin of protein thermostability, J. Mol. Biol. 303 (2000) 125–130.
[4] R.O. Fox, P.A. Evans, C.A. Dobson, Multiple conformations of a protein demonstrated by magnetization transfer NMR spectroscopy, Nature 320 (1986) 192–194.
[5] P.A. Evans, C.M. Dobson, R.A. Kautz, G. Hatfull, R.O. Fox, Proline isomerism in staphylococcal nuclease characterized by NMR and site-directed mutagenesis, Nature 329 (1987) 266–268.
[6] T.A. Alexandrescu, A.P. Hinck, J.L. Markley, Coupling between local structure and global stability of a protein: mutants of staphylococcal nulcease, Biochemistry 29 (1990) 4516–4525.
[7] H. Taniuchi, C.B. Anfinsen, Simultaneous formation of two alternative enzymically active structures by complementation of two overlapping fragments of staphylococcal Nuclease, J. Biol. Chem. 246 (1971) 2291–2301.
[8] C.B. Anfinsen, The formation and stabilization of protein structure, Biochem. J. 128 (1972) 737–749.
[9] G. Jing, B. Zhou, L. Xie, L.J. Liu, Z.G. Liu, Comparative studies of the conformation of the N-terminal fragments of staphylococcal nuclease R in solution, Biochim. Biophys. Acta 1250 (1995) 189–196.
[10] K. Ye, G. Jing, J. Wang, Interactions between subdomains in the partially folded state of staphylococcal nuclease, Biochim. Biophys. Acta 1479 (2000) 123–134.
[11] S. Hirano, K. Mihara, Y. Yamazaki, H. Kamikubo, Y. Imamoto, M. Kataoka, Role of C-terminal region of staphylococcal nuclease for foldability stability and activity, Proteins 49 (2002) 255–265.
[12] C.-Y. Chow, M.-C. Wu, H.-J. Fang, .-K. Hu, H.-M. Chen, T.-Y. Tsong, Compact dimension of denatured states of staphylococcal nuclease, Proteins Struct. Funct. Bioinf. 72 (2008) 901–909.
[13] D. Shortle, A.K. Meeker, Residual structure in large fragments of staphylococcal nuclease: effects of amino acid substitutions, Biochemistry 28 (1989) 936–944.
[14] J.M. Flanagan, M. Kataoka, D. Shortle, D.M. Engelman, Truncated staphylococcal nuclease is compact but disordered, Proc. Natl Acad. Sci. USA 89 (1992) 748–752.
[15] J.M. Flanagan, M. Kataoka, T. Fujisawa, D.M. Engelman, Mutations can cause large changes in the conformation of a denatured protein, Biochemistry 32 (1993) 10359–10370.
[16] A. Lamy, J.C. Smith, Denaturation of truncated Staphylococcal nuclease in molecular dynamics simulation, J. Am. Chem. Soc. 118 (1996) 7326–7328.
[17] B. Zhou, K. Tian, G. Jing, An in vitro peptide folding model suggests the presence of the molten globule state during nascent peptide folding, Protein Eng. 13 (2000) 35–39.
[18] M.R. Eftink, R. Ionescu, G.D. Ramsay, C.Y. Wong, J.Q. Wu, A.H. Maki, Thermodynamics of the unfolding and spectroscopic properties of the V66W mutant of staphylococcal nuclease and its 1–136 fragment, Biochemistry 35 (1996) 8084–8094.
[19] Y.V. Griko, A. Gittis, E.E. Lattman, P.L. Privalov, Residual structure in a staphylococcal nuclease fragment. Is it a molten globule and is its unfolding a first-order phase transition? J. Mol. Biol. 243 (1994) 93–99.
[20] M. Kataoka, K. Kumajima, F. Tokunaga, Y. Goto, Structural characterization of the molten globule of alpha-lactalbumin by solution X-ray scattering, Protein Sci. 6 (1997) 422–430.
[21] Y. Li, G. Jing, Double point mutant F34W/W140F of staphylococcal nuclease is in the molten globule state but highly competent to fold into a functional conformation, J. Biochem. 128 (2000) 739–744.
[22] J. Yin, G. Jing, Tryptophan 140 is important, but serine 141 is essential for the formation of the integrated conformation of staphylococcal nuclease, J. Biochem. 128 (2000) 113–119.
[23] S. Hirano, H. Kamikubo, Y. Yamazaki, M. Kataoka, Elucidation of information encoded in tryptophan 140 of staphylococcal nuclease, Proteins 58 (2005) 271–277.
[24] S. Hirano, H. Kamikubo, K. Mihara, Y. Imamoto, M. Kataoka, The effect of C-terminal deletion on the staphylococcal nuclease studies by solution X-ray scattering, Photon Factory Act. Rep. 17 (2000) 260–270.
[25] J. Kyte, R.F. Doolittle, A simple method for displaying the hydropathic character of a protein, J. Mol. Biol. 157 (1982) 105–132.
[26] Z.-D. Su, J.-M. Wu, H.-J. Fang, T.-Y. Tsong, H.-M. Chen, Local stability identification and role of key aromatic amino acid residue in staphylococcal nuclease folding, FEBS J. 272 (2005) 3960–3966.
[27] S.C. Gill, H. Hippel, Calculation of protein extinction coefficients from amino acid sequence data, Anal. Biochem. 181 (1989) 319–326.
[28] A. Rodger, B. Nordén, Circular Dichroism, Linear Dichoism, University Press Inc., New York, 1997.
[29] K. Nakanishi, N. Berova, R.H. Woody, Circular Dichroism Principles and Applications, VCH publishers, 1994.
[30] T.-Y. Tsong, C.-K. Hu, M.-C. Wu, Hydrophobic condensation and modular assembly model of protein folding, Biosystems 93 (2008) 78–89.
[31] M.R. Eftink, Z. Wasylewski, Time-resolved fluorescence studies of the thermal and guanidine induced unfolding of nuclease A and its unstable mutant. Time-resolved Laser Spectroscopy, Biochem. III 1640 (1992) 579–584.
[32] M.-C. Wu, T.-Y. Tsong, Local hydrophobicity and protein secondary structure formation, Submitted for publication (2010).
[33] K.-W. Leung, Y.-C. Liaw, S.-C. Chan, H.-Y. Lo, F.N. Musayev, J.-Z. Chen, H.-J. Fang, H.-M. Chen, Significance of local electrostatic interactions in staphylococcal nuclease studies by site-directed mutagenesis, J. Biol. Chem. 276 (2001) 46039–46045.